

Second-order amplitudes in loop quantum gravity

Davide Mamone, Carlo Rovelli

Centre de Physique Théorique de Luminy, Case 907, F-13288 Marseille, EU*

(Dated: March 15, 2021)

We explore some second-order amplitudes in loop quantum gravity. In particular, we compute some second-order contributions to diagonal components of the graviton propagator in the large distance limit, using the old version of the Barrett-Crane vertex amplitude. We illustrate the geometry associated to these terms. We find some peculiar phenomena in the large distance behavior of these amplitudes, related with the geometry of the generalized triangulations dual to the Feynman graphs of the corresponding group field theory. In particular, we point out a possible further difficulty with the old Barrett-Crane vertex: it appears to lead to flatness instead of Ricci-flatness, at least in some situations. The observation raises the question whether this difficulty remains with the new version of the vertex.

I. INTRODUCTION

The problem of quantum gravity is—in a sense— a double problem. First, to find the appropriate theory, which we expected to be a background-independent quantum field theory. Second, to learn how to extract physics from such a background-independent quantum field theory. This second problem is highly non-trivial, because most, if not all, of the conventional tools for extracting physics from a quantum field theory rely heavily on the existence of an external metric background.

A tentative solution to this second problem has been developed in the last years [1, 2, 3] and is based on two ingredients. The first is the boundary formalism [4, 5], which we briefly summarize below. The second is the idea of computing transition amplitudes order by order in a background-independent expansion, where the order is given by the number of interaction-vertices, or, equivalently, in the number of n -simplices of the associated dual cellular complex. If the theory is expressed as a group field theory (GFT) [6], this expansion amounts to a perturbative expansion in the GFT coupling constant λ [5]. We denote this expansion the “vertex expansion”, and we discuss below its physical viability.

With only a few exceptions [3, 7], so far most of the literature has been concentrated on first-order terms in this expansion [8, 9, 10, 11, 12]. Here we explore the structure, geometry and physical meaning of some second order terms.¹ The importance of studying higher-order terms is multifold. First, it is not yet clear which is the physical regime where the vertex expansion is good; the easiest way to address the problem is to compare the first-order terms with higher ones. Second, the structure of the expansion is still far from being fully settled: there are open question concerning the correct normalization of the amplitudes, and similar. Again, we think that the best way of addressing these issues is concretely, by studying the terms of the expansion.

The different terms in the vertex expansion that we study have a simple geometrical interpretation. Roughly speaking, the lowest order term can be viewed as describing an approximation to General Relativity where the geometry of the spacetime region under consideration is approximated by a single 4-simplex, of variable shape and size. Higher-order terms give then approximations where the geometry of the region is approximated by a larger number of glued 4-simplices, each of varying shape and size. Here we illustrate in detail the geometry of some cellular complexes contributing to the second-order approximation, obtained by gluing 4-simplices in this way.

We restrict ourselves to computing the *diagonal* part of the propagator, instead of writing its full tensorial structure [10]. Also, we use the dynamics defined by the old Barrett-Crane vertex [13]; in particular, the specific model we use is the theory GFT/B (see [5]), introduced in [14, 15]; the result extends immediately also to the theory GFT/C, introduced in [16], which is characterized by

* Unité mixte de recherche (UMR 6207) du CNRS et des Universités de Provence (Aix-Marseille I), de la Méditerranée (Aix-Marseille II) et du Sud (Toulon-Var); laboratoire affilié à la FRUMAM (FR 2291).

¹ For an analysis of higher order corrections to the quantum gravity propagator in 3 dimensions see [8, 9].

particularly good finiteness properties [17, 18, 19]. For this reason, the results presented here are a bit out-of-date: they need to be extended to the new-vertex models introduced recently [20, 21, 22, 23, 24, 25], which have far better properties. Nothing seems to prevent such extension, and the work done here should open the way for analyzing the theory more of interest. Similarly, the semiclassical behavior considered here needs to be compared with the results on the semiclassical behavior of these new models [26, 27].

We find a certain number of features of the amplitudes, which we summarize in the conclusion section. Of particular interest is the fact that the amplitude appear to be suppressed, at least in some cases, unless the triangulation admits a *flat* metric. This is not what we expect for the classical limit, which should be dominated by *Ricci* flatness. This problem can be a further sign of the difficulties of the old Barrett-Crane model: we think that it needs to be seriously addressed in the context of the new models.

II. PRELIMINARIES

We briefly recall the basis of the formalism that we use. This is not a self sufficient introduction: we refer the reader to [3] for complete definitions and details, and to [5] for a general introduction. On the other hand, we address here and we offer some clarification on some general questions that have been raised concerning the approach.

A. The boundary formalism

The key idea for extracting physics from a background-independent formulation of quantum field theory is to compute transition amplitudes associated with a *finite* spacetime region, as functions of the quantum state on the boundary Σ of the region [1, 4, 5]. In particular, the boundary state will include the quantum state of the of the gravitational field, namely the quantum state of the boundary *geometry*. Physically, this means that we are describing a region of quantum spacetime, as it is observed by apparatuses that take measurements at its boundary — the key point being that these measurements include (quantum) measurements of distances.

If we do so, the information about the background geometry of the region is provided *dynamically* by the (measured) boundary quantum-state itself. Formally, if the boundary geometry determines a classical solution of the Einstein's equations in the bulk, then we expect the Feynman integral in the region to be dominated by configurations around the classical one. In this way, the *interior* background geometry is determined by the *boundary* quantum state: this allows us to define background dependent quantities in the context of a fully background independent bulk theory.

The main tool of this approach is the boundary functional, formally defined by the functional integral over all fields ϕ in the interior region, at fixed boundary value φ

$$W[\varphi] = \int_{\phi|_{\Sigma}=\varphi} D\phi e^{iS[\phi]}. \quad (1)$$

In a background independent theory, where measure $D\phi$ and action $S[\phi]$ are diff-invariant, this quantity does not depend on the spacetime location of Σ . By contracting this quantity with a state $\Psi[\varphi]$, we obtain a probability amplitude associated to this state

$$\langle W|\Psi\rangle \equiv \int D\varphi W[\Sigma] \Psi[\varphi]. \quad (2)$$

This amplitude can then be compared, say, with the amplitude

$$\langle W|\varphi(x)\varphi(y)|\Psi\rangle \quad (3)$$

where $\varphi(x)$ is a field operator creating a quantum excitation over Ψ . The quantity

$$W(x, y; \Psi) = \langle W|\varphi(x)\varphi(y)|\Psi\rangle, \quad (4)$$

where the boundary state Ψ satisfies $\langle \Psi | \Psi \rangle = 1$ and

$$\langle W | \Psi \rangle = 1, \quad (5)$$

gives the probability amplitude for a field's quantum, or a “particle”, to propagate from x to y in the background defined by Ψ (on the meaning of “particle” in this context, see [28]).

This formalism reduces to the standard quantum mechanical formalism on a flat space, if we take Σ to be the union of the two hypersurfaces $t = 0$ and $t = T$, and Ψ to be the element $\Psi_{00} = |0\rangle \otimes \langle 0|$ of the tensor product $\mathcal{H}_{in} \otimes \mathcal{H}_{out}^*$ of the initial and final state spaces [29, 30, 31]. Then, taking $x = (\vec{x}, T), y = (\vec{y}, 0)$,

$$W(x, y; \Psi_{00}) = \langle 0 | \varphi(\vec{x}) e^{-iHT} \varphi(\vec{y}) | 0 \rangle = \langle 0 | \varphi(x) \varphi(y) | 0 \rangle, \quad (6)$$

while the normalization condition (5) is clearly satisfied

$$\langle 0 | e^{-iHT} | 0 \rangle = 1. \quad (7)$$

But the formalism remains meaningful in a diffeomorphism invariant context because the positions y and x of the incoming and outgoing particles are well-defined with respect to the boundary geometry specified by Ψ . That is, $W(x, y; \Psi)$ is not invariant under a coordinate transformation on x and y alone, but it is invariant under a coordinate transformation acting on x, y , as well as Ψ . The *relative* position of the particle with respect to the boundary geometry is diffeomorphism-invariant and the amplitude is therefore well-defined and physically meaningful.

If the background geometry defined by the state Ψ is flat, then the quantity (4) should reduce to the conventional quantum field theoretical two-point function in the weak field limit. In particular, if we compute this quantity in general relativity for the gravitational field, then (4) should reduce to the weak-field graviton propagator

$$W_{\mu\nu\rho\sigma}(x, y; \Psi_{00}) \rightarrow \langle 0 | h_{\mu\nu}(x) h_{\rho\sigma}(y) | 0 \rangle \quad (8)$$

in the large distance limit. The dictionary of the translation between the 3-geometry to 3-geometry transition-amplitude language, and the graviton scattering language, is studied in detail in [32].

B. LQG implementation

The boundary formalism described above can be made concrete in the context of loop quantum gravity (LQG) [33, 34]. We take the state Ψ to live in the LQG state space, and we take the boundary functional given by the spinfoam formalism [5]. The compatibility between the canonical loop-theory and the covariant spinfoam-theory, still unclear when the boundary formalism was developing, has since been firmly established [25]. In particular, a spinfoam dynamics W can be generated by group-field-theoretical methods, where it reproduces the spinfoam model amplitude on any given two-complex, at each order of a vertex expansion [5]. By choosing an s -knot basis $|s\rangle$ in the LQG state space [5], we have then

$$W^{abcd}(x, y, q) = \sum_{ss'} W[s] \langle s' | h^{ab}(x) h^{cd}(y) | s \rangle \Psi_q[s]. \quad (9)$$

for a state satisfying the normalization condition

$$\sum_s W[s] \Psi_q[s] = 1. \quad (10)$$

Concretely, a boundary functional $W[s]$ is defined by any spinfoam model. In fact, a spinfoam model is precisely an algorithm that compute an amplitude $W[s]$ for each boundary spin network s . It has the intuitive interpretation as a regularization of the Misner-Wheeler integral-over-4geometries g

$$W[q] = \int_{g|_{\Sigma}=q} Dg e^{iS_{EH}[g]} \quad (11)$$

intrinsically regularized by the discreteness of the geometry as established by LQG. Here $S_{EH}[g]$ is the Einstein-Hilbert action and q is the boundary 3-geometry.

One possible triangulation independent way to write $W[s]$ is to use GFT [6]. Here we use the Group Field Theory B (GFT-B) spinfoam model

$$W[s] = \int D\phi f_s(\phi) e^{-\int \phi^2 + \frac{\lambda}{5!} \phi^5}. \quad (12)$$

The field ϕ is a function on $SO(4)^4$; s is an s -knot [5] (or, loosely speaking, a “spin network”) with n nodes and f_s is a polynomial of order n in the fields, obtained contracting the indices of the field following the path defined by the s -knot. See [5] for the details and the notation. The choice of this spinfoam model here is dictated only by simplicity and convenience. In fact, the limitations of this model are well known, and the results here need to be extended to the more realistic models.

The Feynman rules of this theory are as follows. The field ϕ decomposes in modes $\phi_{j_n i}^{\alpha_n}$ with $n = 1, 2, 3, 4$. Here j_n are $SU(2)$ representations, α_n is an index in the j_n representation space, and i labels the (elements of a basis in the space of the) intertwiners in the tensor product of the four representation j_n . The standard quantum field theoretical perturbation expansion in λ of this amplitude generates a sum over Feynman graphs with five-valent vertices. The propagator is

$$P_{\alpha_n i \alpha'_n i'}^{j_n^s j_n^s} = \sum_s \mathcal{P}_{\alpha_n i s(\alpha'_n) i'}^{j_n^s s(j_n^s)} \quad (13)$$

where the sum is over all permutations s of four elements and

$$\mathcal{P}_{\alpha_n i \alpha'_n i'}^{j_n^s j_n^s} = \delta_{ii'} \prod_n \delta_{\alpha_n \alpha'_n} \delta^{j_n^s, j_n^s}. \quad (14)$$

The vertex is five-valent, and is given by

$$\mathcal{V}_{\alpha_{nm} i_n}^{j_{nm}} = \lambda \mathcal{B}(j_{nm}) \prod_{n \neq m} \delta_{\alpha_{nm} \alpha_{mn}} \delta^{j_{nm}, j_{mn}} \quad (15)$$

where $\mathcal{B}(j_{nm})$ is the vertex amplitude; see [5]. For large spins, the asymptotic behavior of the vertex amplitude is given by

$$\mathcal{B}(j_{nm}) \sim e^{iS_{\text{Regge}}(j_{nm})} + e^{-iS_{\text{Regge}}(j_{nm})} + D(j_{nm}) \quad (16)$$

where $S_{\text{Regge}}(j_{nm})$ is the Regge action associated to a 4-simplex with areas proportional to j_{nm} and $D(j_{nm})$ is a factor that appears when the areas j_{nm} define degenerate configurations of the 4-simplex. The Regge action has the form

$$S_{\text{Regge}}(j_{nm}) = \sum_{mn} \phi_{nm}(j_{nm}) j_{nm} \quad (17)$$

where $\phi_{nm}(j_{nm})$ are the dihedral angles of the 4 simplices with areas proportional to the j_{nm} .

Each choice of a permutation s at every propagator determines a pattern of contractions of the $\delta_{\alpha\alpha'}$ delta functions; a closed set of contractions $(\delta_{\alpha_1\alpha_2}\delta_{\alpha_2\alpha_3}\dots\delta_{\alpha_n\alpha_1})$ determines a sequence of propagators, and is called a “face”. Thus the sum (13) becomes a sum over the two-complexes with four-valent edges having the Feynman graph as 1-skeleton. In particular, if the two-complex is dual to a 4d triangulation, then the associated amplitude can be shown to be a Feynman sum for a discretization of general relativity on that Regge-like triangulation [22, 25]. Thus, the group field theory generates a discretized Feynman sum for general relativity, where the sum is extended over –appropriately generalized– triangulations [5]. This is why it can be seen as a discretizations of the Misner-Hawking sum-over-4geometries.

C. The vertex expansion

The GFT formulation suggests a perturbative expansion for $W[s]$: the expansion in the GFT coupling constant λ , namely the vertex expansion. The physical meaning of this expansion is clarified by noticing that individual terms of this expansion can be equally obtained by truncating general relativity to the finite-number-of-degrees-of-freedom system formed by a Regge triangulation on a given discretization of spacetime. Notice that is neither a short-scale, nor a large-scale expansion, since the individual 4-simplices can be large or small [22]. It is rather more similar to the approximation used very effectively in cosmology, where only some degrees of freedom of the geometry of the universe are left free [37].

Can such a truncation provide an interesting approximation to the quantum gravitational dynamics? The truncation is background-independent, in the sense in which Regge calculus is. But one may worry that on a fixed triangulation the theory has a finite number of degrees of freedom and therefore it cannot sufficiently capture the field-like behavior of gravity. This objection is wrong, since it would apply to the standard perturbative expansion of QED as well: if we compute a scattering process between a finite number m of particles to a finite order n in perturbative QED, we are restricting the QED Fock space to the subspace formed by a finite number of particle (as many as n vertices can produce from m particles). Thus we are *de facto* truncating QCD to a theory with a finite number of degrees of freedom (a particle has obviously a finite number of degrees of freedom). In other words, conventional QFT perturbation expansion *includes* a truncation of the field theory to a theory with a finite number of degrees of freedom. There is no reason for the same not be viable in gravity.

The correct question, then, is not if the truncation given by the vertex expansion yields a viable approximation, but rather in which regime this approximation is viable. Again, the Regge-lattice analogy provides the answer: any gravitational physics that can be captured by the finite Regge triangulation. For instance if a phenomenon is characterized by a size (wavelength) l and can be confined in a region of size L , then L/l sets the scale of the relevant number of “cells” needed to approximate the phenomenon.

Lattice QCD provides a good example of this: effective lattice QCD calculation yield the correct mass spectrum of the hadrons using lattices that have a rather small number of cells. This number is determined by the ratio between the size of the hadron and the minimal relevant wavelength. What is remarkable is that good quantum physics is obtained with cubic lattices with sides of only a few cells. Clearly there is no really need of infinite lattices to do physics.

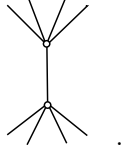
D. The large distance expansion

We are interested in the graviton two-point function (4) at first order in λ , in the limit in which the boundary geometry is large. In this limit we are only looking at very large wavelengths, and it is therefore reasonable to expect that the vertex expansion is viable. The calculation of the graviton two-point function (4) in this limit at first order in λ on the basis of the formalism described above was completed in [2] for the diagonal terms ($\mu = \nu$ and $\rho = \sigma$), and in [10] for the other terms. The fact that the non-diagonal terms of the propagator turned out to be wrong was a main reason for the replacement of the old version of the Barrett-Crane vertex with its new version [20, 22, 23, 25]. The correct $1/L^2$ dependence of the propagator on the distance L , obtained in [2], was confirmed in a next to leading order evaluation [3]. Several second-order terms are considered below.

III. JOINING TWO 4-SIMPLICES

A. One internal propagator: $4 \rightarrow 1 \rightarrow 4$ Pachner's move

Consider the second-order Feynman diagram



Call v^u and v^d (for *up* and *down*) the two vertices of this graph, e the internal propagator, and e_n^u and e_n^d , where $n = 1, 2, 3, 4$ the external legs.

Such a graph can appear in computing the amplitude associated to the observable $f_{s_8}(\phi)$ determined by the spin network s_8 illustrated in Figure 1. The graph of this spin network is Γ_8 . It consists of two tetrahedral spin networks connected by four links. The spin network s_8 is obtained by coloring the links and nodes of Γ_8 . We denote the spins and intertwiners associated with nodes and links of Γ_8 as in Figure 1, Panel b. That is, we denote $j_{nm}^u, j_{nm}^d, j_n^s$ the twenty representations associated with the 20 links $l_{nm}^u, l_{nm}^d, l_n^s$ of Γ_8 , and i_n^u, i_n^d the eight intertwiners associated with the eight nodes n_n^u and n_n^d . The set $s_8 = (\Gamma_8, j_{nm}^u, j_{nm}^d, j_n^s, i_n^u, i_n^d)$ defines a boundary spin network.

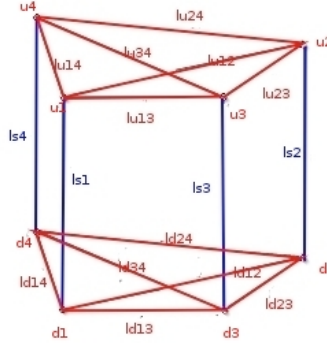


FIG. 1: The boundary spin network s_8 .

The observable $f_{s_8}(\phi)$ determined by this spin network is

$$f_{s_8}(\phi) = \sum_{\alpha_{nm}\beta_{nm}} \prod_{n=1,4} \phi_{j_{nm}^u}^{\alpha_{nm} i_n^u} \phi_{j_{nm}^d}^{\beta_{nm} i_n^d} \quad (18)$$

where we have used the notation $j_{nn}^u := j_{nn}^d := j_n^s$. This is a monomial of order eight in the field. The expansion of its expectation value at order λ^2 gives

$$W[s_8] = \frac{\lambda^2}{2(5!)^2} \int D\phi f_{s_8}(\phi) \left(\int \phi^5 \right)^2 e^{-\int \phi^2} \quad (19)$$

The Wick expansion of this integral gives two vertices and nine propagators. (If d is the order of ϕ in f_s , and n_v is the number of vertices, then the number of propagators is clearly $n_p = \frac{d+5n_v}{2}$). In particular, consider the term where the four *up* (resp. *down*) legs of the graph are connected to the upper (resp. lower) tetrahedral spin network, as in Figure 2; the corresponding amplitude is

$$W[s_8] = \left(\prod_{n=1,4} P_{\alpha_{nm}\alpha_n i_n^u}^{j_{nm}^u j_n^u} \right) \mathcal{V}_{\alpha'_{nm}\gamma_m i'_n i''}^{j'_{nm} j''_{nm}} P_{\gamma_m i''}^{j'_m j''_m} \mathcal{V}_{\delta_m i''' \beta'_n i'_n}^{j'''_{nm} j''_{nm}} \left(\prod_{n=1,4} P_{\beta_{nm}\beta_n i_n^d}^{j_{nm}^d j_n^d} \right). \quad (20)$$

In the first parenthesis we have the contribution from the *up* boundary (contractions among the “up” four boundary tetrahedra u_n); then we have the contraction between these and the fifth (taken as “internal”); then the internal propagator; then the down vertex and the contractions in the ‘down’ boundary.

The sums over permutations (13) in the propagators give rises to a sum over two-complexes having the Feynman graph as two-skeleton. Since we are interested in the large j behavior of the amplitude, and since each face of the two-complex carries some powers of j , the dominant term will be the one with the maximum number of faces. It is not hard to see that this term is given by the term

$$\begin{aligned} W[s_8] &= \left(\prod_{n=1,4} \mathcal{P}_{\alpha_{nm}\alpha_n i_n^u}^{j_{nm}^u j_n^u} \mathcal{P}_{\alpha'_{nm} i_n^d}^{j_{nm}^d j_n^d} \right) \mathcal{V}_{\alpha'_{nm} \gamma_m i_n^u}^{j_{nm}^u j_m^u} \mathcal{P}_{\gamma_m i''}^{j_m^u j_m^d} \mathcal{V}_{\delta_m i'''}^{j_m^d j_{nm}^d} \mathcal{V}_{\delta_m i'''}^{j_m^d j_{nm}^d} \left(\prod_{n=1,4} \mathcal{P}_{\beta_{nm}\beta_n i_n^d}^{j_{nm}^d j_n^d} \mathcal{P}_{\beta'_{nm} i_n^u}^{j_{nm}^u j_n^u} \right) \\ &= \left(\prod_{n=1,4} \dim(i_n^u) \dim(i_n^d) \dim(j_n) \right) \left(\prod_{n < m, n=1,4} \dim(j_{nm}^u) \dim(j_{nm}^d) \right) \mathcal{B}(j_{nm}) \mathcal{B}(j_{nm}) \quad (21) \end{aligned}$$

of the sum over permutations. Let us analyze this term. It is obtained by adding sixteen faces to the Feynman graph: four faces f_n bounded by the three edges e_n^u, e, e_n^d , six faces f_{nm}^u bounded by the two edges e_n^u and e_m^u and six faces f_{nm}^d bounded by the two edges e_n^d and e_m^d . The nodes n_n^u and n_n^d of Γ_8 bound the edges e_n^u and e_n^d respectively. The links l_n^s, l_{nm}^u and l_{nm}^d of this graph bound the faces f_n, f_{nm}^u and f_{nm}^d , respectively.

The structure of this two-complex becomes transparent by noticing that it is the complex dual to a rather simple triangulation, which we call Δ_8 . This is obtained by gluing two 4-simplices by one tetrahedron \mathcal{T} . The four-dimensional triangulation Δ_8 is illustrated in the first panel of Fig. 3. This is the 4d analog of the 3d and 2d cases illustrated in the other two panels of the figure.

The triangulation Δ_8 is formed by 6 points, which we label as $1, 2, 3, 4, u, d$; by the 14 edges $(n, m), (n, u), (n, d)$; the 12 faces $(n, m, n), (n, m, u), (n, m, d)$; the 9 tetrahedra $(1, 2, 3, 4), (n, m, p, u), (n, m, p, d)$ and the two 4-simplices $(1, 2, 3, 4, u), (1, 2, 3, 4, d)$. Here $n = 1, 2, 3, 4$ and $n \neq m \neq p$.

The two vertices v^u and v^d are dual to the two 4-simplices of this triangulation. The four triangles that bound \mathcal{T} are the dual to the faces f_n ; the other six triangles of the upper (resp. lower) 4-simplex are dual to the faces f_{nm}^u (resp. f_{nm}^d). Notice that all these triangles belong to the boundary of the triangulation, as is clear from the 3d analog. The graph dual to this boundary is clearly the Γ_8 graph of Figure 1: the four upper nodes of Γ_8 correspond to the four upper tetrahedra; the four lower nodes of Γ correspond to the four lower tetrahedra. The six links joining the upper (lower) nodes correspond to the six upper (lower) vertical triangles t_{nm}^u (t_{nm}^d); the four vertical links correspond to the four triangles t_n bounding \mathcal{T} . Therefore Γ_8 is the dual of a triangulation of a compact 3d surface, with the topology of a three-sphere, which can be viewed as the boundary of the spacetime region formed by two adjacent 4-simplices.

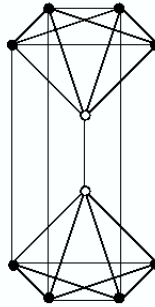


FIG. 2: Feynman graph and boundary spinnetwork

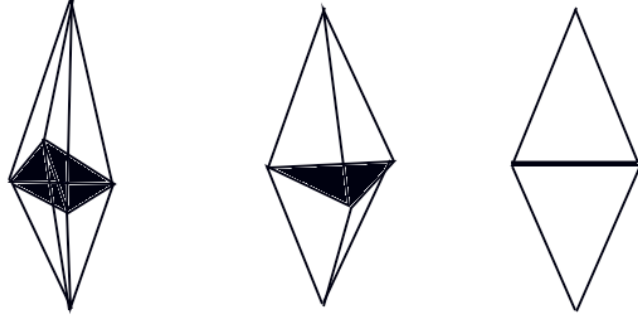


FIG. 3: The spacetime triangulation Δ_8 and the 3d and 2d analogs.

The path of the indices in (21) gives the geometrical decomposition of the triangulation illustrated in Fig.4, where each line corresponds to a face of the two complex, or, equivalently, a triangle of the triangulation.

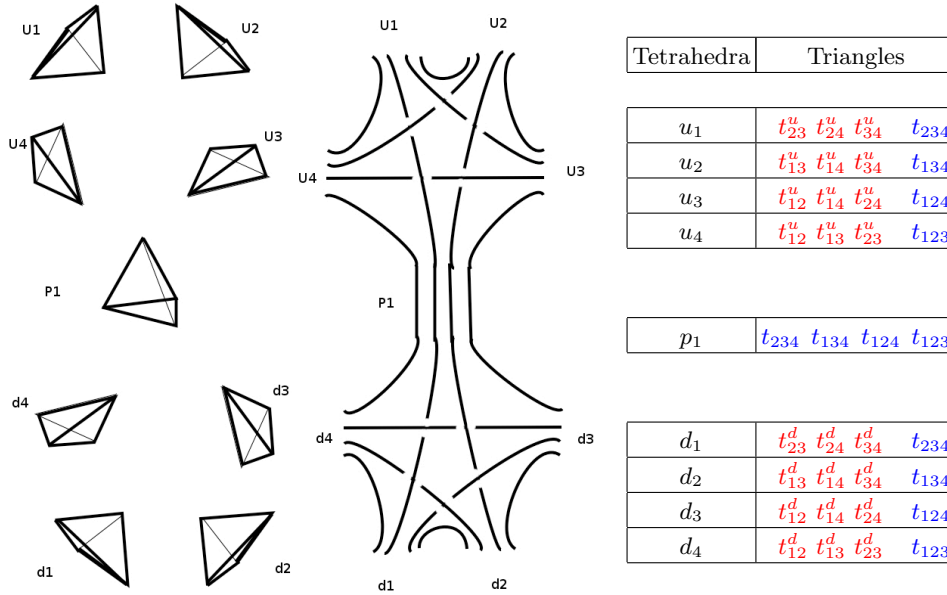


FIG. 4: a: *Tetrahedral decomposition*: the up 4-simplex (tetrahedra $u_1 u_2 u_3 u_4 p_1$) is glued to the down 4-simplex ($p_1 d_1 d_2 d_3 d_4$) through the shared tetrahedron p_1 . b: *GFT diagram*: every line corresponds to a triangle, four lines grouped to a tetrahedron. c: Relation between tetrahedra and triangles.

If we interpret the vertical axis as a “time” axis, the triangulation Δ_8 represents the world-history of a point d opening up to a tetrahedron \mathcal{T} and then recollapsing to a point u . (In the 3d case, we have a point opening up to a triangle and then recollapsing; in the 2d case, we have a point opening up to a segment and then recollapsing. See Fig.3.) The process described by this amplitude can therefore be interpreted as a creation and annihilation of an “atom of space” [3].

Following [3], let us now use the amplitude (21) for computing a contribution to the graviton two-point function, at given boundary state. At this order, the relevant component of the boundary state is on the graph Γ_8

$$\Psi_{\mathbf{q}}[s_8] = \Psi_{\mathbf{q}}(j_{nm}^{u,d}, j_n^s). \quad (22)$$

Let us assume that the boundary state describes a regular semiclassical geometry for the boundary of the triangulation Δ_8 . Let this be peaked on the geometry \mathbf{q}_8 defined by the the boundary of the region of R^4 formed by the two pyramidal 4-simplices having for basis a regular tetrahedron \mathcal{T} with side of length L' , and height T . Since we are interested in the large j regime, we peak the state on the values

$$j_n^{s(8)} = \frac{\sqrt{3}}{32\pi\hbar G} L'^2 \equiv j_L, \quad (23)$$

$$j_{nm}^{u(8)} = j_{nm}^{d(8)} = \frac{1}{8\pi\hbar G} \left(2L' \sqrt{\frac{L'^2}{8} + T^2} + \frac{\sqrt{3}}{2} L'^2 \right) \equiv j_{TL}. \quad (24)$$

We do not give here the explicit value of the background dihedral angles $\Phi_l^{(8)}$, which can be obtained by elementary geometry: for details see appendix in [3]. We choose a boundary state given by a

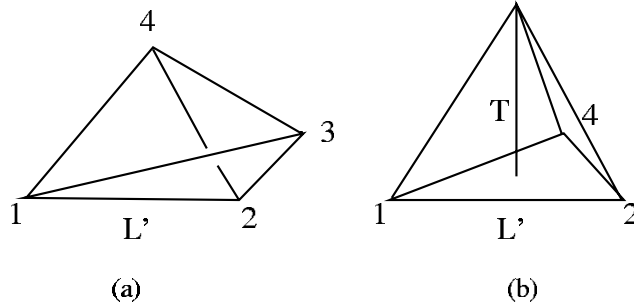


FIG. 5: Central tetrahedron (a). Lateral tetrahedron (b).

Gaussian peaked on \mathbf{q}_8 . Writing all spins in a single vector $j_l = (j_{nm}^u, j_{nm}^d, j_n^s)$, we have

$$\Psi_{\mathbf{q}}[s_8] = C_8 e^{-\alpha_{l'} (j_l - j_l^{(8)}) (j_{l'} - j_{l'}^{(8)}) + i \Phi_l^{(8)} j_l}. \quad (25)$$

Following [2, 3], we contract the four indices of (9) with normals to boundary triangles, and choose in particular, say, to look at the “diagonal” term determined by the triangles t_{12}^u and t_{13}^d , obtaining

$$\mathbf{G}_{s_8}(L', T) \equiv (n_{12}^u)_a (n_{12}^u)_b (n_{13}^d)_c (n_{13}^d)_d W^{abcd}(x, y, \mathbf{q}_8) = \sum_{ss'} W[s] \langle s' | \delta j_{12}^u \delta j_{23}^d | s \rangle \Psi_q[s] \quad (26)$$

where $\delta j = j - j^{(8)}$. All the terms in this expression are now well defined.

We now use the asymptotic expression for each \mathcal{B} , as in [2]. This is given by the cosine of the Regge action plus the degenerate term. The phase in the boundary state suppresses the sum unless it is matched by a corresponding phase of a term in $W[s]$. This happens for only one of the exponentials in the cosine, as can be seen as follows. The sum of the Regge actions for the two 4-simplices, $S_{\text{Regge}} = S_{\text{Regge}}^u + S_{\text{Regge}}^d$ can be expanded around j_{TL} and j_L

$$S_{\text{Regge}}(j_{nm}^u, j_{nm}^d, j_n^s) = \tilde{\phi}_{nm}^{(8)} j_{nm}^u + \tilde{\phi}_n^{(8)} j_n^s + \tilde{\phi}_{nm}^{(8)} j_{nm}^d + \tilde{\phi}_n^{(8)} j_n^s + \frac{1}{2} G_{ll'} \delta j_l \delta j_{l'}, \quad (27)$$

where $\tilde{\phi}_n^{(8)}$ and $\tilde{\phi}_{nm}^{(8)}$ are the dihedral angles of flat 4-simplices with the given boundary *intrinsic* geometry; the linear terms in the expansion of the Regge action sum up, giving the dihedral angle of the boundary of the 4d region, which is precisely the sum of the dihedral angles of the two 4-simplices at the faces of \mathcal{T} . That is, $\tilde{\phi}_{nm}^{(8)} = \Phi_{nm}^{(8)}$, but $2\tilde{\phi}_n^{(8)} = \Phi_n^{(8)}$. The second order term in (27) is the “discrete derivative” [3]

$$G_{ll'} = \left(\frac{\delta^2 S_{\text{Regge}}}{\delta j_l \delta j_{l'}} \right)_{j_l = j_l^{(8)}}. \quad (28)$$

This matrix can be computed from elementary geometry. Being a derivative of an angle with respect of an area, $G_{ll'}$ should scale as the inverse of $\sqrt{j_l^{(8)} j_{l'}^{(8)}}$. It is therefore convenient to define the scaled quantity

$$\Gamma_{ll'} = \frac{G_{ll'}}{\sqrt{j_l^{(8)} j_{l'}^{(8)}}}. \quad (29)$$

Thus, we obtain

$$\mathbf{G}_{ss}(L', T) = \frac{4\lambda^2 \mathcal{N}_8}{j_{TL}^2} \sum_{\delta j_l} \delta j_{12}^u \delta j_{13}^d P_\tau^2 e^{-i(S_{Regge}^u + S_{Regge}^d + k_\tau \frac{\pi}{2})} e^{-\tilde{\alpha}_{ll'}(j_l - j_l^{(8)})(j_{l'} - j_{l'}^{(8)}) + i\Phi^{(8)} j_l} \quad (30)$$

where \mathcal{N}_8 is fixed by the normalization condition. If only the Feynman graph that we are considering enters it, we have

$$\frac{1}{\mathcal{N}_8} = \frac{4\lambda^2}{j_{TL}^2} \sum_{\delta j_l} P_\tau^2 e^{-i(S_{Regge}^u + S_{Regge}^d + k_\tau \frac{\pi}{2})} e^{-\tilde{\alpha}_{ll'}(j_l - j_l^{(8)})(j_{l'} - j_{l'}^{(8)}) + i\Phi^{(8)} j_l} \quad (31)$$

The Gaussian peaks the sums around the background values. We can therefore expand the summand around these values. The first order term of the expansion of the Regge action around these values cancels the phases in the state, leaving

$$\mathbf{G}_{ss}(L', T) = \frac{4\mathcal{N}_8 \lambda^2}{j_{TL}^2} \sum_{\delta j_l} \delta j_{12}^u \delta j_{13}^d e^{-\frac{1}{2} \delta \mathbf{j}^T \tilde{\mathcal{A}} \delta \mathbf{j}}, \quad (32)$$

where we have introduced the matrix

$$\tilde{\mathcal{A}}_{ll'} = 2\tilde{\alpha}_{ll'} + iG_{ll'} = \sqrt{j_l^{(0)} j_{l'}^{(0)}} (2\alpha + i\Gamma)_{ll'} = \sqrt{j_l^{(0)} j_{l'}^{(0)}} \mathcal{A}_{ll'} \quad (33)$$

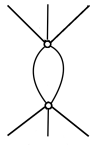
and the vector $\delta \mathbf{j} = (\delta j_l) = (\delta j^u, \delta j^d, \delta j^s)$. Approximating the sum with gaussian integrals gives

$$\mathbf{G}_{ss}(L', T) = \frac{16\pi}{j_{TL}^2} (\tilde{\mathcal{A}})^{-1}_{j_{12}^u, j_{13}^d} = \frac{16\pi}{j_{TL}^2} (\mathcal{A})^{-1}_{j_{12}^u, j_{13}^d} \quad (34)$$

which is proportional to $1/j_L$, as in the first order calculation [2]. Thus we recover the expected $\frac{1}{L^2}$ behavior of the linearized theory.

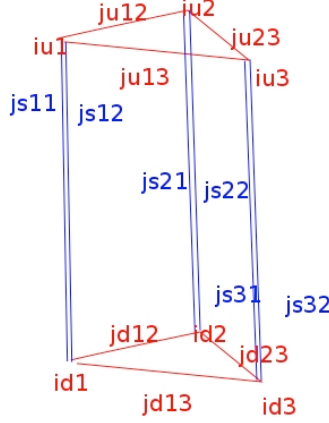
B. Two internal propagators: $3 \rightarrow 2 \rightarrow 3$ Pachner's move

Consider the Feynman diagram



This will appear in the amplitude of an observable f_{s_6} defined by a spin network with graph Γ_6 , illustrated in Fig.6, consisting of two triangular spin networks connected by six links: three “up” nodes u_n , and three “down” nodes d_n , $n = 1, 2, 3$.

It is convenient to denote the links of this spin network as follows. Call l_{nm}^u (resp l_{nm}^d) with $n \neq m$ and $n, m = 1, 2, 3$ the three upper (resp. lower) links, and denote l_{nv}^s with $v = 4, 5$ the two links joining u_n and d_n . Denote $j_{nm}^u, j_{nm}^d, j_{nv}^s$ the representations associated to the 12 links $l_{nm}^u, l_{nm}^d, l_{nv}^s$ of Γ_6 , and

FIG. 6: The boundary spin network s_6 .

i_n^u, i_n^d the six intertwiners associated to the six nodes n_n^u and n_n^d . The set $s_6 = (\Gamma_6, j_{nm}^u, j_{nm}^d, j_{nv}^s, i_n^u, i_n^d)$ is the boundary spin network we consider in this section.

The boundary function $f_{s_6}(\phi)$ for this spin network is a monomial of order six in the field:

$$f_{s_6}(\phi) = \sum_{\{\alpha\}} \prod_{n=1,2,3} \phi_{j_{nm}^u j_{nv}^s}^{\alpha_{nm}^u i_n^u} \phi_{j_{nm}^d j_{nv}^s}^{\alpha_{nm}^d i_n^d} \quad (35)$$

where $n \neq m = 1, \dots, 5$. At order λ^2 , the corresponding amplitude

$$W[s_6] = \frac{\lambda^2}{2(5!)^2} \int D\phi f_{s_6}(\phi) \left(\int \phi^5 \right)^2 e^{-\int \phi^2} \quad (36)$$

gives two vertices and eight propagators:

$$W[s_6] = \left(\prod_{n=1,3} \mathcal{P}_{\alpha_{nm} \alpha_n i_n^u}^{j_{nm}^u j_n} \mathcal{P}_{\alpha'_{nm} i_n^u}^{j'_{nm}} \right) \mathcal{V}_{\alpha'_{nm} \gamma_{nm} \eta_{nm} i_n^u i_n^u i_n^u i_n^u}^{j'_{nm} j''_{nm} j'''_{nm}} \mathcal{P}_{\gamma_{nm} i_n^u}^{j''_{nm}} \mathcal{P}_{\delta_{nm} i_n^u}^{j'''_{nm}} \quad (37)$$

$$\times \mathcal{P}_{\eta_{nm} i_n^u}^{j''_{nm}} \mathcal{P}_{\theta_{nm} i_n^u}^{j'''_{nm}} \mathcal{V}_{\theta_{nm} i_n^u i_n^u i_n^u i_n^u}^{j''_{nm} j'''_{nm} j''_{nm} j'''_{nm}} \mathcal{P}_{\delta_{nm} i_n^u}^{j''_{nm}} \mathcal{P}_{\beta'_{nm} i_n^u}^{j'''_{nm}} \left(\prod_{n=1,3} \mathcal{P}_{\beta_{nm} \beta_n i_n^d}^{j_{nm}^d j_n} \mathcal{P}_{\beta'_{nm} i_n^d}^{j''_{nm}} \right)$$

As before, the two complex with the highest number of faces is the one with \mathcal{P} replaced by P . This is dual to the (generalized) triangulation Δ_6 , obtained by gluing two 4-simplices via two tetrahedra. This is schematically indicated in Figure 7.

The triangulation Δ_6 is formed by 5 points, which we label as 1, 2, 3, 4, 5; by the 11 edges $(n, m), (n, 4), (n, 5), (4, 5)_u, (4, 5)_d$ (here $n = 1, 2, 3$; notice that there are *two* distinct edges connecting the points 4 and 5); the 13 faces $(1, 2, 3), (n, m, 4), (n, m, 5), (n, 4, 5)_u, (n, 4, 5)_d$; the 8 tetrahedra $(1, 2, 3, 4), (1, 2, 3, 5), (n, m, 4, 5)_u, (n, m, 4, 5)_d$ and the two 4-simplices $(1, 2, 3, 4, 5)_u, (1, 2, 3, 4, 5)_d$.

We use also the notation $p_4 \equiv (1, 2, 3, 4)$ and $p_5 \equiv (1, 2, 3, 5)$ for these two tetrahedra, $\mathcal{T}_2 = p_4 \cup p_5$ their union, and $\tau \equiv (1, 2, 3)$ the triangle that separates them. The triangulation can be interpreted as representing the world-history of the line $(4, 5)_d$ opening up to the volume \mathcal{T}_2 , and then recollapsing to the line $(4, 5)_u$. The initial and final line join at both ends. See Figure 8 and Figure 9.

We use also the notation $t_{nm4} \equiv (n, m, 4)$, $t_{nm5} \equiv (n, m, 5)$, and the notation $t_1^{u,d} \equiv (2, 3, 4, 5)_{u,d}$, $t_2^{u,d} \equiv (3, 1, 4, 5)_{u,d}$, $t_3^{u,d} \equiv (1, 2, 4, 5)_{u,d}$ (cyclically in 1, 2, 3). The tetrahedra in the triangulation Δ_6 and their relations are represented in Fig.10.

For this term, we have

$$W[s_6] = \sum_j \dim(j) \prod_{n < m} \dim(j_{nm}^u) \dim(j_{nm}^d) \dim(j_{n4}^s) \dim(j_{n5}^s) \mathcal{B}(j, j_{nm}^u, j_{nv}^s) \mathcal{B}(j, j_{nm}^d, j_n^s). \quad (38)$$

Notice the sum over the spin j of the internal face. This sum is finite, because it is controlled by the Clebsch-Gordan relations between spins at the edges.

The vacuum boundary state $\Psi_{\mathbf{q}}[s_6]$ for spin network s_6 will be a function $\Psi_{\mathbf{q}}[s_6]$ peaked on background values $(j_{nm}^{u,d(6)}, j_{nv}^{s(6)})$ which represent a given background geometry \mathbf{q}_6 . Notice that we cannot imbed two flat non-degenerate 4-simplices glued along *two* faces into R^4 (for the same reason for which two non-degenerate triangles in R^2 cannot be glued along *two* sides). Thus, we cannot fix the geometry \mathbf{q}_6 as we did in the previous case. Instead, let us proceed as follows.

Let v_u and v_d be two regular 4-simplices, of side L . Identify two tetrahedra (p_4 and p_5) of these two 4-simplices. This defines a conical space that is flat except on the triangle τ that separates p_4 and p_5 , where the deficit angle is 2π minus twice the dihedral angle of a regular 4-simplex. This space has a fixed boundary geometry, which we take as the definition of \mathbf{q}_6 .

We take the boundary state to be a Gaussian peaked on \mathbf{q}_6 :

$$\Psi_{\mathbf{q}}[s_6] = C_6 e^{-\alpha_{ll'}(j_l - j_l^{(6)})(j_{l'} - j_{l'}^{(6)}) + i\Phi_l^{(6)} j_l}. \quad (39)$$

Following the same steps as above, we found now that the Regge action is now also a function of the summation variable j_{45} , which represents the area of the internal triangle τ .

$$\begin{aligned} S_{Regge}(j_{nm}^u, j_{nm}^d, j_n^l, j_n^r, j) &= \tilde{\phi}_{nm}^{(6)} j_{nm}^u + \tilde{\phi}_n^{(6)} j_{n,v}^s + \tilde{\phi}_{nm}^{(6)} j_{nm}^d + \tilde{\phi}_n^{(6)} j_{n,v}^s + \\ &+ \frac{1}{2} G_{ll'} \delta j_l \delta j_{l'} + G_{(45)l'} \delta j_{45} \delta j_{l'} + \\ &+ (\tilde{\phi}_{45}^{u(6)} + \tilde{\phi}_{45}^{d(6)}) j_{45} + \frac{1}{2} G_{(45)(45)} \delta j_{45} \delta j_{45}, \end{aligned} \quad (40)$$

where $\tilde{\phi}_n^{(6)}$ and $\tilde{\phi}_{nm}^{(6)}$ are the dihedral angles of flat 4-simplices with the given boundary geometry and are supposed to be function of the reference background value $j_{45}^{(6)}$, like the “discrete derivative” and the fluctuation $\delta j_{45} = j_{45} - j_{45}^{(6)}$. Since we have an internal loop we sum over δj_{45}

$$\mathbf{G}_{s_6}(L', T) = \frac{4\Lambda^2 \mathcal{N}_6}{j_{TL}^2} \sum_{\delta j_l} \sum_{\delta j_{45}} \delta j_l^u \delta j_{l'}^d P_\tau^2 e^{-i(S_{Regge} + k_\tau \frac{\pi}{2})} e^{-\tilde{\alpha}_{ll'}(\delta j_l)(\delta j_{l'}) + i\Phi_l^{(6)} j_l} \quad (41)$$

where \mathcal{N}_6 is fixed by the normalization. The first order term of the expansion of the Regge action cancels the phases in the boundary state but gives an extra phase $i(\tilde{\phi}_{45}^{(6)u} + \tilde{\phi}_{45}^{(6)d})j_{45}$ and two discrete

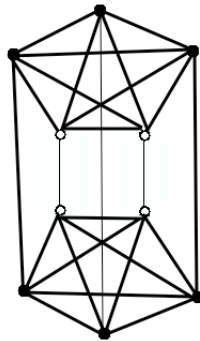


FIG. 7: Gluing two 4-simplices via two tetrahedra. Dots represent the tetrahedra; lines represent triangles. The empty dots connected by a thin line are identified. The lines emerging from connected empty dots are identified as well.

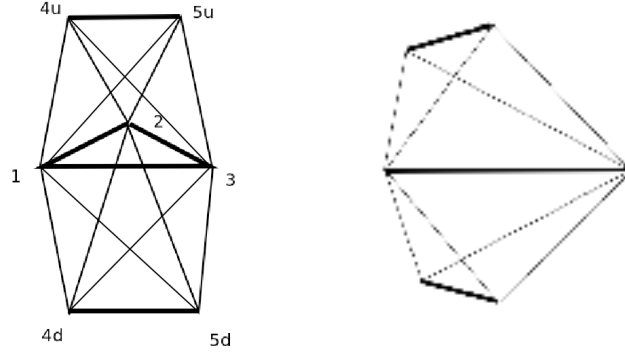


FIG. 8: a): The spacetime triangulation Δ_6 . The point $5u$ and $5d$ must be identified, and so the points $4u$ and $4d$. The triangles $2-3-5u$ must be identified with the triangle $2-3-5d$, and so on. The line $4u-5u$ must *not* be identified with the line $4d-5d$. b): The 3d analog of Δ_6 ; here as well the two ends of the upper horizontal line must join the two ends of the lower horizontal line, and the two side triangles of the upper tetrahedron must be identified with the two side triangles of the lower tetrahedron.

derivative terms $G_{(45)l}$ and $G_{(45)(45)}$ related to the internal loop, leaving

$$\begin{aligned} \mathbf{G}_{s_6}(L', T) = & N_6 \sum_{\delta j_l} \sum_{\delta j_{45}} \delta j_l^u \delta j_{l'}^d \exp \left(-\tilde{\alpha}_{ll'} \delta j_l \delta j_{l'} - \frac{i}{2} G_{ll'} \delta j_l \delta j_{l'} + \right. \\ & \left. + i(\tilde{\phi}_{45}^{(6)u} + \tilde{\phi}_{45}^{(6)d}) j_{45} + G_{(45)l'} \delta j_{45} \delta j_{l'} + \frac{1}{2} G_{(45)(45)} \delta j_{45} \delta j_{45} \right) \end{aligned} \quad (42)$$

The dihedral angle $\tilde{\phi}_{45}^{(6)u}$ are the angles between the normals of the two internal tetrahedra (p_1 and p_2) in the two 4-simplices. Their sum is the deficit angle at the triangle \mathcal{T}_2 . As mentioned, this deficit angle cannot be zero (or a multiple of 2π), because there is no imbedding of two nondegenerate 4-simplices glued by *two* tetrahedra into R^4 . Therefore

$$\tilde{\phi}_{45}^{(6)u} + \tilde{\phi}_{45}^{(6)d} \neq 0. \quad (43)$$

But it follows from this that the sum over δ_{45} is a sum of a rapidly oscillating function, and is therefore suppressed. Thus, this term is strongly suppressed in the large j limit. Notice that the denominator might also be suppressed at this order in λ , but is not going to be suppressed at all orders in λ ; therefore the suppression is effective.

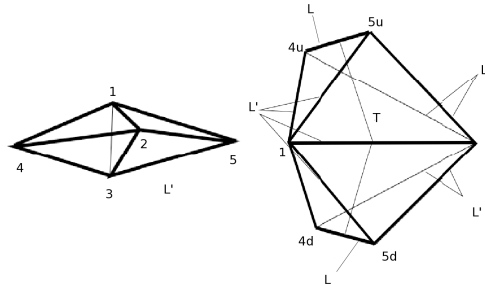


FIG. 9: The labeling of the vertices of the central tetrahedra (a) and the lateral tetrahedra (b).

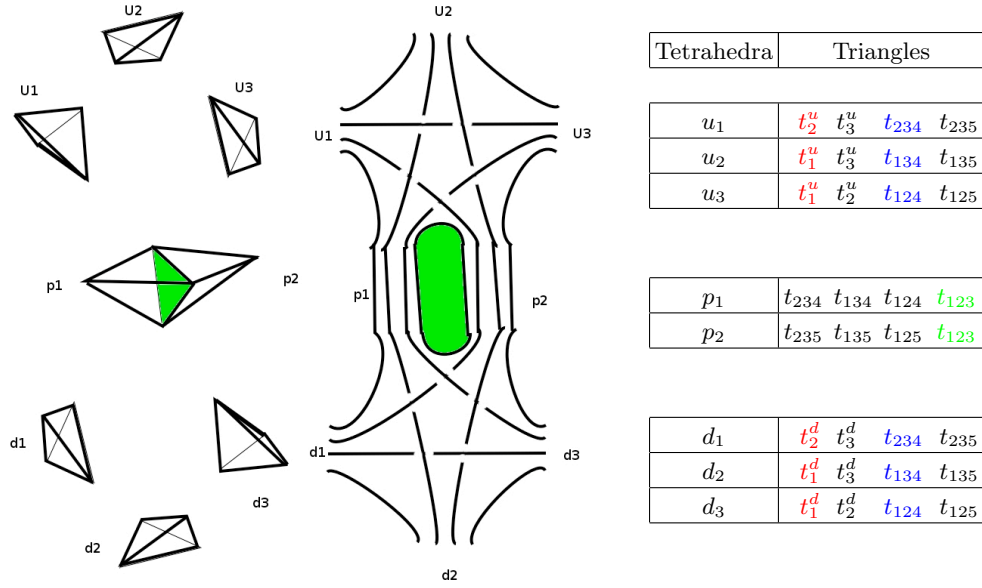
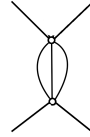


FIG. 10: *Tetrahedral decomposition*: a) two 4-simplices share two tetrahedra p_1 and p_2 . b) *GFT diagram*: 3 up and 3 down boundary lines, 6 propagators lines and 1 internal loop (green). c) 3 boundary up u_n tetrahedra share 6 (blue) triangles with 3 down tetrahedra d_n .

C. Three internal propagators: $2 \rightarrow 3 \rightarrow 2$ Pachner's move

Consider the Feynman graph



The boundary graph Γ_4 is illustrated in Fig.11: two theta spin networks connected by two links.

Denote the nodes of the first link as u_1 and u_2 and the nodes of the second one as d_1 and d_2 . The generalized triangulation Δ_4 that gives the maximal contribution is obtained by gluing two 4-simplices

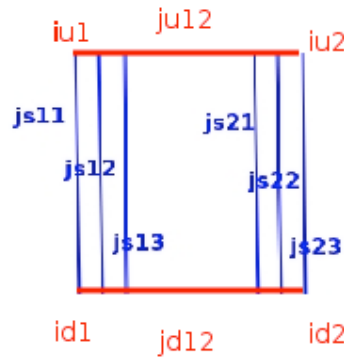


FIG. 11: The boundary spin network s_4 .

via *three* tetrahedra. See Figure 13.

The triangulation Δ_4 is formed by 5 points, which we label as 1, 2, 3, 4, 5; by the 10 edges $(n, m), (n, 1), (n, 2), (1, 2)$ (here $n = 3, 4, 5$); the 11 faces $(n, m, 1), (n, m, 2), (n, 1, 2), (3, 4, 5)_u, (3, 4, 5)_d$ (notice that there are two distinct *triangles* connecting the points 3, 4 and 5); the 7 tetrahedra $(n, m, 1, 2), (3, 4, 5, 1)_u, (3, 4, 5, 2)_u, (3, 4, 5, 1)_d, (3, 4, 5, 2)_d$; and the two 4-simplices $(1, 2, 3, 4, 5)_u, (1, 2, 3, 4, 5)_d$. See Figure 12.

We use the notation $p_3 = (4, 5, 1, 2), p_4 = (5, 3, 1, 2), p_5 = (3, 4, 1, 2)$ and we call $\mathcal{T}_3 = p_3 \cup p_4 \cup p_5$ the union of the three central tetrahedra. The triangulation Δ_4 can be seen as the world-history of the triangle $(3, 4, 5)_d$ evolving in to \mathcal{T}_3 and then recollapsing into the triangle $(3, 4, 5)_u$. The initial and final triangles share their perimeters, and in particular their vertices.

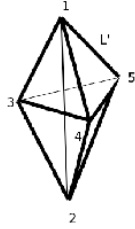


FIG. 12: Labelling of the vertices of Δ_4 .

The representations associated to the 8 links $l_{12}^u, l_{12}^d, l_{nv}^s$ of Γ_4 are $j_{12}^u, j_{12}^d, j_{nv}^s$ while i_n^u, i_n^d are the four intertwiners associated to the four nodes u_n and d_n ($n = 1, 2$). The set $s_4 = (\Gamma_4, j_{12}^u, j_{12}^d, j_{nv}^s, i_n^u, i_n^d)$ is the boundary spin network we consider in this section. The boundary function $f_{s_4}(\phi)$ is of order four

$$f_{s_4}(\phi) = \sum_{\alpha_{nm}\beta_{nm}} \prod_{n=1,2} \phi_{j_{nm}^u}^{\alpha_{nm}i_n^u} \phi_{j_{nm}^d}^{\beta_{nm}i_n^d} \quad (44)$$

and the expansion gives two vertices and seven propagators:

$$\begin{aligned} W[s_4] &= \left(\prod_{n=1,2} \mathcal{P}_{\alpha_{nm}\alpha_n i_n^u}^{j_{nm}^u j_n} \mathcal{P}_{\alpha'_{nm}\alpha'_n i'_n}^{j'_{nm} j'_n} \right) \mathcal{V}_{\alpha'_{nm}\gamma_m \eta_m i'_n i'' i^{IV} i^{VI}}^{j'_{nm} j'_m j_m^{IV} j_m^{VI}} \mathcal{P}_{\gamma_m i''}^{j'_m j'_m} \mathcal{P}_{\gamma_m i^{IV}}^{j'_m j'_m} \mathcal{P}_{\gamma_m i^{VI}}^{j'_m j'_m} \\ &\times \mathcal{P}_{\eta_m i^{VI}}^{j'_m j'_m} \mathcal{P}_{\theta_m i^{VII}}^{j'_m j'_m} \mathcal{V}_{i^{VII}\theta_m i^{VI} \delta_m i^{III} \beta'_{nm} i'_n}^{j'_m j'_m j'_m j'_m} \left(\prod_{n=1,2} \mathcal{P}_{\beta_{nm}\beta_n i_n^d}^{j_{nm}^d j_n} \mathcal{P}_{\beta'_{nm}\beta'_n i'_n}^{j'_{nm} j'_n} \right) \\ &= \prod_{n=1,2} \dim(i_n^u) \dim(i_n^d) \prod_{v=1,3} \dim(j_{n,v}) \dim(j_{12}^u) \dim(j_{12}^d) \sum_{j_{kl}} \left(\prod_{k=3,4} \dim(j_{kl}) \right) \mathcal{B}(j_{nm}^{(4)}) \mathcal{B}(j_{nm}^{(4)}) \end{aligned} \quad (45)$$

where the I label of j_I refer to the three internal faces shared by the tetrahedra, along which they are glued together (loops in the GFT diagram).

We now chose a boundary geometry with nondegenerate areas and dihedral angles, defining nondegenerate 4-simplices. Let $j_l = (j_{12}^u, j_{12}^d, j_{nv}^s)$ be the background values on which the boundary function $\Psi_{\mathbf{q}}[s_4]$ is peaked:

$$\Psi_{\mathbf{q}}[s_4] = C_4 e^{-(\alpha_4)_{ll'}(j_l - j_l^{(4)})(j_{l'} - j_{l'}^{(4)}) + i\Phi_l^{(4)} j_l} \quad (46)$$

and $(j_{nm}^{u,d(4)}, j_n^{s(4)})$ the areas of the internal faces determined by the boundary geometry. The Regge action, as before, will be written as an expansion over the boundary j_l but also over the internal background reference $j_{34}^{(4)}, j_{35}^{(4)}$ and $j_{45}^{(4)}$:

$$\begin{aligned} S_{\text{Regge}}(j_{nm}^u, j_{nm}^d, j_{n,v}^s, j_{IJ}) &= \tilde{\phi}_{nm}^{(4)} j_{nm}^u + \tilde{\phi}_n^{(4)} j_{n,v}^s + \tilde{\phi}_{nm}^{(4)} j_{nm}^d + \tilde{\phi}_n^{(4)} j_{n,v}^s + \\ &+ \frac{1}{2} G_{ll'} \delta j_l \delta j_{l'} + i \left(\tilde{\phi}_{IJ}^{u(4)} + \tilde{\phi}_{IJ}^{d(4)} \right) j_{IJ} + \\ &+ G_{(IJ)\nu} \delta j_{IJ} \delta j_{\nu} + \frac{1}{2} G_{(IJ),(KL)} \delta j_{IJ} \delta j_{KL} \end{aligned} \quad (47)$$

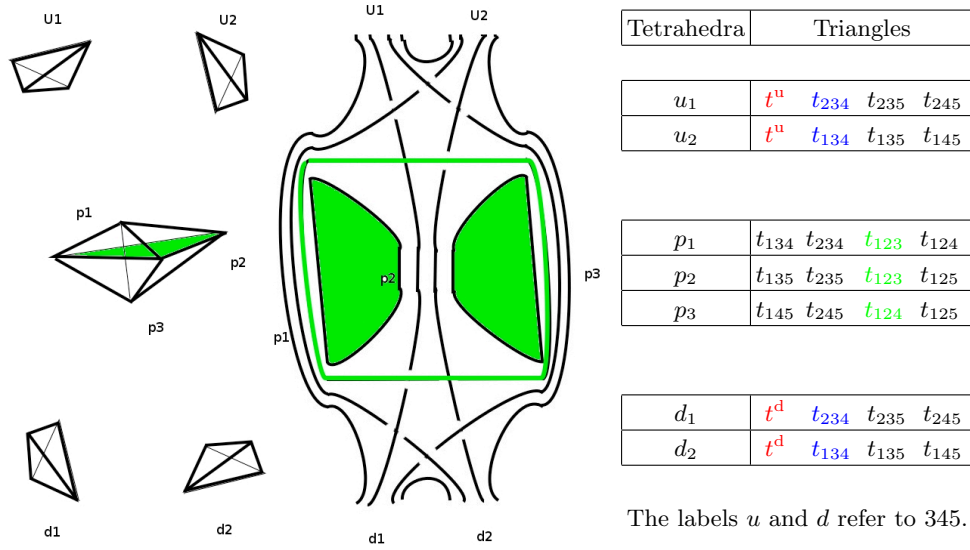


FIG. 13: *Tetrahedral decomposition*: two 4-simplices share three tetrahedra p_1 , p_2 and p_3 .

where $I, J, K, L = 3, 4, 5$, $I < J$, $K < L$, $\tilde{\phi}_{n,v}^{(4)}$ and $\tilde{\phi}_{nm}^{(4)}$ are the dihedral angles.

The phases of the external angles cancel the phases in the boundary state. The phases in the internal angles are

$$\left(\tilde{\phi}_{34}^{(4)u} + \tilde{\phi}_{34}^{(4)d}\right)j_{34}^4 + \left(\tilde{\phi}_{35}^{(4)u} + \tilde{\phi}_{35}^{(4)d}\right)j_{35}^4 + \left(\tilde{\phi}_{45}^{(4)u} + \tilde{\phi}_{45}^{(4)d}\right)j_{45}^4 = 0 \quad (48)$$

The sum over the three independent variables j_{34}, j_{45}, j_{53} suppresses again the amplitude, because the deficit angles in the parenthesis cannot vanish, for the same reason as in the previous section.

However, this result raise a problem. We expect contributions in a Feynman sum to be suppressed in the semiclassical approximation if there is no classical trajectory that give a saddle point in the sum. Here the classical trajectories should reproduce the Einstein equations, and these demand the Ricci tensor to vanish, and not the Riemann tensor. But the vanishing of all deficit angles above correspond to to flatness, namely to the vanishing of the Riemann tensor. Why don't (non-flat) Ricci-flat configurations contribute in the semiclassical limit?

The origin of the problem can be traced to the oversimplification of the dynamics which characterizes the old Barrett-Crane vertex. In this model, the spins are the sole dynamical variables. In the semiclassical limit, they correspond to areas of triangles of Regge-like triangulations. The vertex approximates correctly the Regge action, but this is not sufficient to reproduce the Regge-calculus dynamics, because the variables are areas instead of lengths. On this, see [36]. Let's see how this problem reflects here.

We are considering a (generalized) triangulation obtained by gluing two 4-simplices by three tetrahedra. The segments of this triangulation are 10, because all segments are shared by the two 4-simplices. But the areas are 11, because only 9 triangles are shared, and each 4-simplex has a triangle which is not shared with the other 4-simplex. Therefore there should be one relation among the areas to be satisfied if the areas have to define a geometrical (Regge-like) generalized triangulation. Of these 11 areas, 8 are boundary areas, and three are internal. If we fix the 8 external areas, there should be a relation between the three internal areas. Suppose we linearize this relation

$$a\delta j_{34} + b\delta j_{45} + c\delta j_{53} = 0 \quad (49)$$

and impose this in the integral of δj_{nm} . Then the integral is not anymore suppressed, provided that the deficit angle angles satisfy a relations like

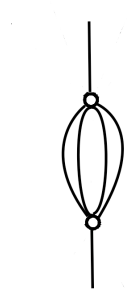
$$\left(\tilde{\phi}_{34}^{(4)u} + \tilde{\phi}_{34}^{(4)d}\right) = a\phi, \quad \left(\tilde{\phi}_{45}^{(4)u} + \tilde{\phi}_{45}^{(4)d}\right) = b\phi, \quad \left(\tilde{\phi}_{53}^{(4)u} + \tilde{\phi}_{53}^{(4)d}\right) = c\phi. \quad (50)$$

That is, the amplitude may fail to be suppressed even if the triangulation is not flat. It is reasonable to expect that the above condition reflects Ricci flatness.

In the model we are considering, a relation between the fluctuations of the spins does not seem to be implemented; and this is perhaps one additional sign of the problems of the old Barrett-Crane model. Do the new models correct this problem?

D. Four internal propagators: $1 \rightarrow 4 \rightarrow 1$ Pachner's move

Finally, consider the Feynman graph



which looks like a self-energy correction for the GFT propagator. The potential divergences of this graph have been analyzed in [7] in the simple case of vanishing boundary areas.

The boundary graph Γ_2 is dual to the spinnetwork of Fig.14: a tetrahedral spin network with two nodes u_1 and d_1 . The links of Γ_2 are the four side links l_n^s , which connect u_1 with d_1 .

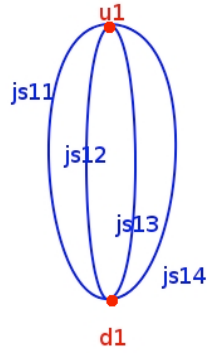


FIG. 14: The boundary spin network s_2 .

The corresponding maximal four-dimensional triangulation Δ_2 is made by two 4-simplices glued by *four* tetrahedra.

The triangulation Δ_2 is formed by 5 points, which we label as 1,2,3,4,5; by the 10 edges $(n,m), (n,5)$ (here $n = 1,2,3,4$); the 10 faces $(n,m,n), (n,m,5)$; the 6 tetrahedra $(n,m,p,5), (1,2,3,4)_u, (1,2,3,4)_d$ (notice that there are two distinct *tetrahedra* connecting the points 1, 2, 3 and 4); and the two 4-simplices $(1,2,3,4,5)_u, (1,2,3,4,5)_d$. See Figure 15.

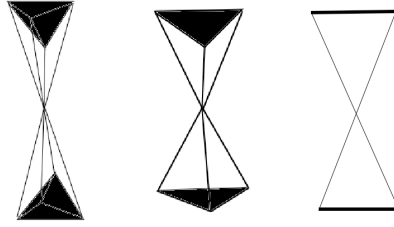


FIG. 15: The spacetime triangulation Δ_2 and the lower dimensional analogies. Upper and lower lateral side must be identified.

This can be seen as the world-history of the tetrahedron $d \equiv (1, 2, 3, 4)_d$ evolving into a set of four tetrahedra, having the same 3d boundary of original one, and then evolving back to a single tetrahedron $u \equiv (1, 2, 3, 4)_u$.

The *boundary* of Δ_2 is made by two tetrahedra (Fig.III D): “up” tetrahedron u_1 and “down” d_1 . They share all their four faces, that is, the triangles t_{234} , t_{235} , t_{245} , t_{345} . See Figure 16.

Denote j_v^s ($v = 1, 4$) the spins associated to the 4 links l_n^s of Γ_2 , and i_1^u, i_1^d the two intertwiners associated to the two nodes u_1 and d_1 . The set $s_2 = (\Gamma_2, j_v^s, i_1^u, i_1^d)$ with $v = 1, 2, 3, 4$ is the boundary spin network. The boundary function $f_{s_2}(\phi)$ is of order two

$$f_{s_2}(\phi) = \sum_{\alpha_{nm}\beta_{nm}} \phi_{j_{nm}^u}^{\alpha_{nm}i_1^u} \phi_{j_{nm}^d}^{\beta_{nm}i_1^d} \quad (51)$$

The Wick expansion of the highest dimensional contribution gives two vertices and six propagators

$$\begin{aligned} W[s_2] &= \mathcal{V}_{\alpha'_{nm}\gamma_m\eta_m i'_n}^{j'_{nm} j_m^{II} j_m^{IV} j_m^{VI} j_m^{VIII}} \mathcal{P}_{\gamma_m i^{II}}^{j_m^{II}}, \frac{j_m^{III}}{\delta_m i^{III}} \\ &\quad \times \mathcal{P}_{\gamma_m i^{IV}}^{j_m^{IV}}, \frac{j_m^V}{\delta_m i^V} \mathcal{P}_{\eta_m i^{VI}}^{j_m^{VI}}, \frac{j_m^{VII}}{\theta_m i^{VII}} \mathcal{P}_{\eta_m i^{VIII}}^{j_m^{VIII}}, \frac{j_m^{IX}}{\theta_m i^{IX}} \mathcal{V}_{i^{IX} i^{VII} \theta_m i^V \delta_m i^{III} \beta'_n i'_n}^{j_m^{VII} j_m^V j_m^{III} j_m^{II}} \\ &= (\dim i_1^u \dim i_1^d) \left(\prod_{v=1,4} \dim(j_{1v}) \right) \sum_{j_{KL}} \left(\prod_{K=2,3,4,5; K < L} \dim(j_{KL}) \mathcal{B}(j_{nm}) \mathcal{B}(j_{nm}) \right) \end{aligned} \quad (52)$$

Let us choose again the boundary geometry that defines the boundary state $\Psi_{\mathbf{q}}[s_2]$ as the one obtained by gluing regular simplices.

$$\Psi_{\mathbf{q}}[s_2] = C_2 e^{-(\alpha_2)_{ll'}(j_l - j_l^{(2)})(j_{l'} - j_{l'}^{(2)}) + i\Phi_l^{(2)} j_l}. \quad (53)$$

Notice that something new happens with this amplitude, which did not happen in the previous cases: In general, the amplitude is suppressed unless the first order expansion of the Regge action matches the phases of the boundary state. This gives a certain number of conditions on the internal spins (since these determine the dihedral angle appearing in the Regge action). Now, in the previous cases these conditions were sufficient to determine (the value around to which to expand) the internal spins uniquely. But this is not anymore true in the present case. Indeed, there are four external triangles, and therefore four conditions for the cancellation of the four phases Φ_l in (53), while there are *six*

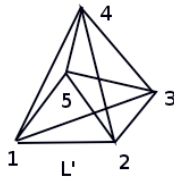
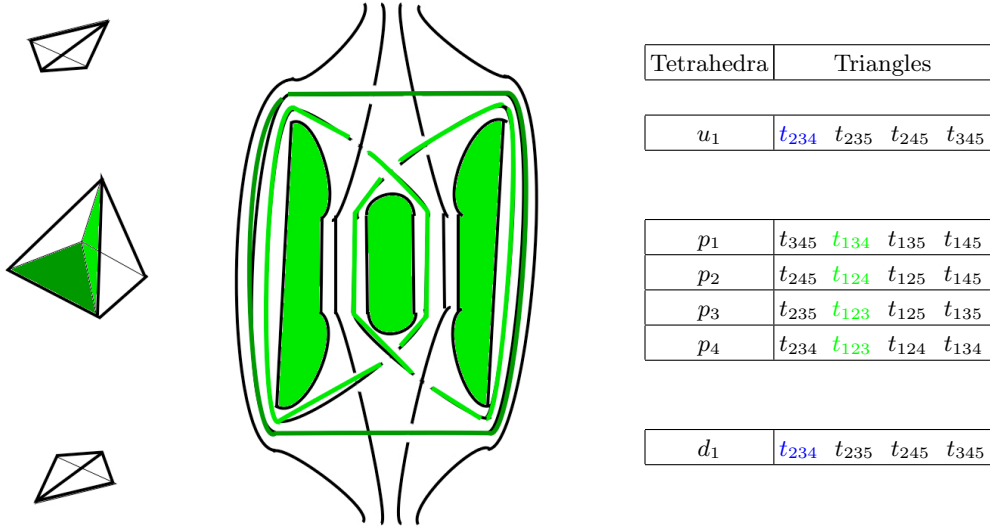


FIG. 16: The labeling of the vertices of the triangulation Δ_2 .

FIG. 17: The tetrahedral decomposition of the $1 \rightarrow 4 \rightarrow 1$ diagram.

internal faces. Therefore we can expect a two-parameter set of internal spins, whose contribution to the amplitude is *not* suppressed by boundary-phase cancellation.

On the other hand, there are six *internal* deficit angles that appear in the expansion of the Regge action around the boundary j_l and the internal references $j_{IJ}^{(2)}$, with $I < J$ and $I, J = 2, 3, 4, 5$, where now $j_l = (j_{1v}^s)$, with $v = 1, 4$ and $I, J, K, L = 2, 3, 4, 5$, $I < J$, $K < L$

$$S_{\text{Regge}}(j_n^s, j_{IJ}) = \tilde{\phi}_n^{(2)} j_{1v}^s + \frac{1}{2} G_{ll'} \delta j_l \delta j_{l'} + \tilde{\phi}_n^{(2)} j_{1v}^s + (\tilde{\phi}_{IJ}^{(2)u} + \tilde{\phi}_{IJ}^{(2)d}) j_{IJ} + \quad (54)$$

$$+ G_{(IJ)l'} \delta j_{IJ} \delta j_{l'} + \frac{1}{2} G_{(IJ),(KL)} \delta j_{IJ} \delta j_{KL},$$

and the give unmatched phases

$$\sum_{I,J=2,3,4,5; I < J} \left(\tilde{\phi}_{IJ}^{(2)u} + \tilde{\phi}_{IJ}^{(2)d} \right) j_{IJ}^2. \quad (55)$$

Thus, it appears that this terms is suppressed as well. However, we expect this term to have a divergence, due to the presence of a bubble; does the divergence show in this large j limit?

E. Subleading corrections

Remarkably, none of the λ^2 terms considered here appear to give just a second order corrections in $1/j$ to the propagator. The first case we have considered, namely the $4 \rightarrow 1 \rightarrow 4$ case, which is not suppressed, gives a contribution at the leading $1/j$ order. (This would happens for the other terms as well if we disregard the exponential suppression factor.) Notice that in this case there is no first order term for a boundary state that has only support on the graph Γ_8 .

Of course terms of higher orders in $1/j$ abound as contributions to the amplitude. First, we have expanded the vertex amplitude in $1/j$: all the vertex subleading terms will contribute to the amplitude. More interestingly, recall that the propagator of the GFT includes the sum over permutations (13). We have systematically considered only the term with the highest power in j of this sum. The other terms give lower powers in j .

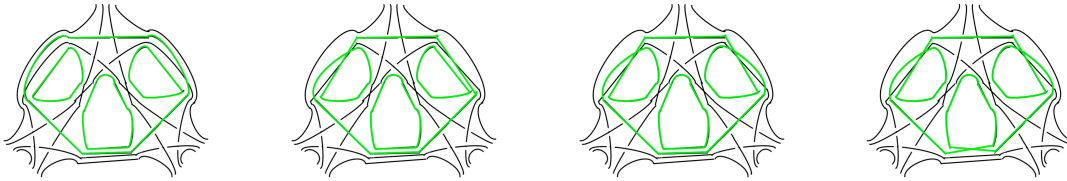


FIG. 18: Different permutations in the propagators give a different number of faces: an example.

Notice in fact that the same sum over permutations appear in the normalization of the amplitude which is fixed by (11). The dominant term of the normalization will always be the one with highest power in j , and therefore the other terms in the amplitude will contribute as increasing powers in $1/j$. It is tempting to speculate that these terms are probably to be interpreted as related to the corrections of the Newton potential, in agreement with standard correction obtained with quantum-field-theoretical techniques discussed in the literature (see [38, 39])

$$V(r) = a_1 \frac{Gm_1m_2}{r} \left(1 + a_2 \frac{G(m_1 + m_2)}{c^2} \frac{1}{r} + a_3 \left(\frac{G\hbar}{c^3} \right)^2 \frac{1}{r^2} \right) + \dots \quad (56)$$

with a_1 , a_2 and a_3 numerical coefficients. The actual calculation of these coefficients using the techniques developed here, however, requires more work, of which the one presented here is only a first step.

IV. CONCLUSIONS

We have explored some second-order contributions to the loop quantum gravity scattering amplitudes. Our results are preliminary, and a more extensive study of these terms is needed. Some general considerations appear nevertheless to be possible, and some interesting phenomena have appeared.

- i. Second order terms do not appear to spoil the correct large distance behavior of the two-point function.
- ii. The dominant contribution for the terms considered here appear to come from the two-complex with the maximal number of faces, which minimizes the complexity of the topology of its dual triangulation. In other words, triangulations with very funny topologies appear to contribute less, at large distance.
- iii. Terms of higher order in λ contribute to the dominant $1/j$ term of the propagator, a result perhaps unexpected, but that was already pointed out in [3]. (This is the result of the $1 \rightarrow 4 \rightarrow 1$ case.)
- iv. The amplitude is suppressed unless the triangulation admits configurations where internal deficit angles appropriately vanish. Thus, triangulations that admit only geometries that cannot solve the (discretized) Einstein equations do not contribute in the large j limit. (This is the result of the $2 \rightarrow 3 \rightarrow 2$ case.)
- v. Apparently, however, only triangulations that admit a flat geometry seem not to be suppressed. This appears to be a problem, since it is *Ricci* flatness, which seems the physically reasonable requirement. This might be a problem of the model that we have used, and we think it should be clarified in the context of the new models [20, 22, 23, 25]. (This is the result of the $3 \rightarrow 2 \rightarrow 3$ case.)
- vi. When the bulk of the triangulation is sufficiently more complex than the boundary, the internal spins are not fixed by the boundary geometry. The consequences of this case on the semiclassical limit are not yet clear to us. (This is the result of the $4 \rightarrow 1 \rightarrow 4$ case.)

- vii. Finally, it is not clear to us what happens in the large j limit to the bubble divergence which is expected in the $4 \rightarrow 1 \rightarrow 4$ case.

Many other aspects of the problem remain unclear. Among the most important, are how to work with general boundary states with components on different graphs, and to understand which one is the physical regime where the expansion in powers of λ is viable. We think that continuing a concrete systematical exploration of the amplitudes may be useful path for addressing these questions.

Thanks to Eugenio Bianchi for numerous useful comments.

The work of D.M. was partially supported by Fondazione Della Riccia and by EGIDE program of the French embassy in Italy.

-
- [1] L Modesto, C Rovelli: “Particle scattering in loop quantum gravity”, *Phys Rev Lett* 95 (2005) 191301
 - [2] C Rovelli: “Graviton propagator from background-independent quantum gravity”, *Phys Rev Lett* 97 (2006) 151301
 - [3] E Bianchi, L Modesto, C Rovelli, S Speziale: “Graviton propagator in loop quantum gravity”, *Class Quant Grav* 23 (2006) 6989-7028
 - [4] R Oeckl, “A ‘general boundary’ formulation for quantum mechanics and quantum gravity”, *Phys Lett B* 575 (2003) 318-324; “Schrödinger’s cat and the clock: lessons for quantum gravity”, *Class Quant Grav* 20 (2003) 5371-5380
 - [5] C Rovelli, *Quantum Gravity*, (Cambridge University Press, Cambridge, 2004)
 - [6] D Oriti, in “Mathematical and Physical Aspects of Quantum Gravity”, B Fauser, J Tolksdorf and E Zeidler, eds., Birkhaeuser, Basel (2006) gr-qc/0512103. L Freidel, “Group Field Theory: an overview”, *Int Journ Theor Phys* 44 (2005) 1769-1783. L Freidel, J P Ryan, “Spin Foam Models: The Dynamics Of Quantum Geometry,” *Class Quant Grav* 25 (2008) 114004.
 - [7] C Perini, C Rovelli, S Speziale: “Self-energy and vertex radiative corrections in LQG”, arXiv:08101714
 - [8] S Speziale, “Towards the graviton from spinfoams: the 3d toy model”, gr-qc/0512102
 - [9] E Livine, S Speziale, J Willis, “Towards the graviton from spinfoams: higher order corrections in the 3d toy model”, *Phys Rev D* 75 (2007) 024038. V Bonzom, E Livine, M Smerlak, S Speziale, *Nucl Phys B* 804: (2008) 507-526
 - [10] E Alesci, C Rovelli: “The complete LQG propagator: I. Difficulties with the Barrett-Crane vertex”, *Phys Rev D* 76 (2007) 104012
 - [11] E Alesci, C Rovelli: “The complete LQG propagator: II. Asymptotic behavior of the vertex”, *Phys Rev D* 77 (2008) 044024
 - [12] E Alesci, E Bianchi, C Rovelli, “LQG propagator: III. The new vertex,” arXiv:0812.5018.
 - [13] JW Barrett, L Crane, *Relativistic spin networks and quantum gravity*, *J Math Phys* 39 (1998) 3296.
 - [14] R DePietri, L Freidel, K Krasnov, C Rovelli, “Barrett-Crane model from a Boulatov-Ooguri field theory over a homogeneous space”, *Nucl Phys B* 574 (2000) 785
 - [15] D Oriti, RM Williams, “Gluing 4-simplices: a derivation of the Barrett-Crane spinfoam model for Euclidean quantum gravity”, *Phys Rev D* 63 (2001) 024022
 - [16] A Perez, C Rovelli, *Nucl Phys B* 599 (2001) 255-282,
 - [17] A Perez, “Finiteness of a spinfoam model for euclidean GR”, *Nucl Phys B* 599 (2001) 427-434.
 - [18] A Perez, C Rovelli, “A spinfoam model without bubble divergences”, *Nucl Phys B* 599 (2001) 255-282
 - [19] L Crane, A Perez, C Rovelli: “Finiteness in spinfoam quantum gravity”, *Physical Review Letters* 87 (2001) 181301.
 - [20] J Engle, R Pereira, C Rovelli: “The loop-quantum-gravity vertex-amplitude”, *Phys Rev Lett* 99 (2007) 161301
 - [21] ER Livine, S Speziale, “A new spinfoam vertex for quantum gravity,” *Phys Rev D* 76 (2007) 084028. ER Livine, S Speziale, “Consistently Solving the Simplicity Constraints for Spinfoam Quantum Gravity” *Europhys Lett* 81 (2008) 50004
 - [22] J Engle, R Pereira, C Rovelli: “Flipped spinfoam vertex and loop gravity”, *Nucl Phys B* 798 (2008) 251-290
 - [23] L Freidel, K Krasnov, “A New Spin Foam Model for 4d Gravity”, *Class Quant Grav* 25 (2008) 125018
 - [24] R Pereira, “Lorentzian LQG vertex amplitude,” *Class Quant Grav* 25 (2008) 085013
 - [25] J Engle, R Pereira, C Rovelli: “LQG vertex with finite Immirzi parameter”, *Nucl Phys B* 799 (2008) 136-149

- [26] J W Barrett, R J Dowdall, W J Fairbairn, H Gomes, F Hellmann, “Asymptotic analysis of the EPRL four-simplex amplitude,” arXiv:0902.1170.
- [27] F Conrady, L Freidel, “Path integral representation of spin foam models of 4d gravity,” *Class Quant Grav* 25 (2008) 245010. F Conrady, L Freidel, “Quantum geometry from phase space reduction,” arXiv:0902.0351.
- [28] D Colosi, C Rovelli, “What is a particle?,” *Class Quant Grav* 26 (2009) 025002 (old title: “Global particles, local particles”).
- [29] F Conrady, L Doplicher, R Oeckl, C Rovelli, M Testa, “Minkowski vacuum in background independent quantum gravity,” *Phys Rev D* 69 (2004) 064019
- [30] F Conrady, C Rovelli “Generalized Schrödinger equation in Euclidean field theory”, *Int J Mod Phys A* 19, (2004) 1-32.
- [31] L Doplicher, “Generalized Tomonaga-Schwinger equation from the Hadamard formula,”, *Phys Rev D* 70 (2004) 064037
- [32] F Mattei, C Rovelli, S Speziale, M Testa, “From 3-geometry transition amplitudes to graviton states,” *Nucl Phys B* 739 (2006) 234–253,
- [33] C Rovelli, L Smolin, “Knot theory and quantum gravity”, *PRL* 61 (1988) 1155; C Rovelli, L Smolin, “Loop space representation for quantum general relativity”, *Nucl Phys B* 331 (1990) 80. C Rovelli, L Smolin, “Discreteness of Area and Volume in Quantum Gravity”, *Nucl Phys B* 442 (1995) 593; B456 (1995) 734. C Rovelli, “Loop quantum gravity and black hole physics”, *Helv Phys Acta* 69 (1996) 582
- [34] Ashtekar A, Lewandowski J 1997, “Quantum Theory of Geometry I: Area Operators” *Class and Quantum Grav* 14(1997) A55; “II : Volume Operators”, *Adv Theo Math Phys* 1(1997) 388-429
- [35] JC Baez, “An introduction to spin foam models of BF theory and quantum gravity,” *Lect Notes Phys* 543 (2000) 25; “Spin foam models,” *Class Quant Grav* 15 (1998) 1827. M Reisenberger, C Rovelli, “Spacetime as a Feynman diagram: The connection formulation,” *Class Quant Grav* 18, 121 (2001) M Reisenberger and C Rovelli, “Spin foams as Feynman diagrams” in *Florence 2001, A relativistic spacetime odyssey* pg 431-448. A Perez, “Spin Foam Models for Quantum Gravity”, *Class and Quantum Grav* 20 (2003) R43
- [36] B Dittrich, L Freidel, S Speziale, “Linearized dynamics from the 4-simplex Regge action,” *Phys Rev D* 76 (2007) 104020
- [37] C Rovelli, F Vidotto, “Stepping out of Homogeneity in Loop Quantum Cosmology,” *Class. Quant. Grav.* 25 (2008) 225024.
- [38] HW Hamber, S Liu, “On the Quantum Corrections to the Newtonian Potential”, *Physics Letters B* 357 (1995) 51
- [39] JF Donoghue, “Leading Quantum Correction to the Newtonian Potential”, *Phys Rev Lett* 72 (1994) 2996.